# Reactions of Laser-Ablated Osmium and Ruthenium Atoms with Nitrogen. Matrix Infrared Spectra and Density Functional Calculations of Osmium and Ruthenium Nitrides and Dinitrides

**Angelo Citra and Lester Andrews***

*Department of Chemistry, University of Virginia, Charlottesville, Virginia 22901*

*Received: September 17, 1999; In Final Form: November 15, 1999*

Laser-ablated osmium and ruthenium atoms were reacted with nitrogen molecules; the products were isolated in solid argon and nitrogen and identified by infrared spectroscopy. Both MN and NMN nitrides are observed, and estimates for the triatomic bond angles are made using nitrogen and ruthenium isotopic data. The growth of NOsN on annealing in solid argon suggests that osmium atoms insert into the dinitrogen triple bond at cryogenic temperatures, allowing a lower limit of ∼473 kJ/mol to be estimated for the average Os−N bond energy in NOsN. The force constants for MN and NMN (M= Fe, Ru, Os) were calculated using all available isotopic data; force constants increase moving down the metal group, and diatomic MN force constants are larger than those for the corresponding NMN triatomic molecules. DFT calculations for the ruthenium and osmium nitrides give reasonable agreement with experiment. Bonding analyses for these molecules show that the M−N bonds are largely nonpolar with bond orders in the range 2.5−3.0. Several metal dinitrogen complexes are also observed and assignments are proposed.

## Introduction

Osmium and ruthenium have an extensive nitrido and dinitrogen chemistry. Species of the form $OsNX_5^{2-}$ and $OsNX_4^-$ (X = Cl, Br, I) are known, and they undergo a variety of reactions, including the abstraction of sulfur from thiocyanate and substitution by phosphine ligands.[1] These species contain strong Os−N bonds with significant multiple bond character, as shown by the bond lengths and stretching frequencies. The analogous ruthenium nitrides have been characterized.[1] Various dinitrogen complexes are also known for both metals, the most notable of these is $[Ru(NH_3)N_2]^{2+}$ which was the first stable dinitrogen complex to be isolated.[2] The analogous osmium complex $[Os(NH_3)N_2]^{2+}$ is a useful synthetic intermediate.[3] The interaction between the metal surfaces and nitrogen has also been studied with regard to their effectiveness in ammonia synthesis.[4−6]

In this work, osmium and ruthenium nitrides and dinitrogen complexes are formed by the reaction of the respective metal atoms with dinitrogen and are isolated in argon and nitrogen matrixes at cryogenic temperatures. The reaction products are characterized using infrared spectroscopy and density functional theory, and the results are discussed within the context of the previous matrix isolation study of iron nitrides in this laboratory.[7]

## Experimental Section

The technique for laser ablation and FTIR matrix investigation has been described previously.[8,9] Osmium (E-VAC Products, 99.98%, hot pressed) and ruthenium (Goodfellow Metals, 99.9%) metal targets were mounted on a rotating (1 rpm) stainless steel rod. The Nd:YAG laser fundamental (1064 nm, 10 Hz repetition rate, 10 ns pulse width, 40−50 mJ pulses) was focused on the target through a hole in the CsI cryogenic window (maintained at 7−8 K by a Displex refrigerator). Metal atoms were co-deposited with $^{14}N_2$ and $^{14}N_2 + {}^{15}N_2$ in argon (4%) at 5−8 mmol/h for 60−90 min, and with undiluted $^{14}N_2$ and $^{14}N_2 + {}^{15}N_2$ for 30 min at the same rate. FTIR spectra were recorded with 0.5 $cm^{-1}$ resolution on a Nicolet 550 instrument. Matrix samples were successively warmed and recooled, and more spectra were collected; the matrix was subjected to broad-band photolysis with a medium-pressure mercury arc (Philips, 175 W) with globe removed (240−580 nm) at different stages in the annealing cycles.

## Results and Discussion

Infrared spectra and density functional theory (DFT) calculations of osmium and ruthenium dinitrogen reaction products will be presented in turn. The osmium and ruthenium nitride spectra in the frequency ranges 1140−860 $cm^{-1}$ and 1000−800 $cm^{-1}$ are shown in Figures 1 and 2, respectively. The first spectrum in Figure 1 shows osmium in a pure nitrogen isotopic mixture $^{14}N_2 + {}^{15}N_2$ after the first annealing cycle, and the remaining spectra show the annealing behavior for similar samples diluted in argon matrixes. The spectra in Figure 2 for ruthenium in mixed isotope nitrogen matrixes clearly show the natural ruthenium isotopic structure. Absorptions due to the osmium and ruthenium dinitrogen complexes are observed above 2000 $cm^{-1}$ and are shown in Figures 3 and 4, respectively, for osmium and ruthenium with $^{14}N_2 + {}^{15}N_2$. Figures 5 and 6 show the corresponding $^{14}N_2$ argon matrix experiments with osmium and ruthenium, respectively. All absorptions and isotopic counterparts are listed in Tables 1−4.

Density functional theory in the Gaussian 98 program was employed to calculate structures and frequencies for ruthenium and osmium nitride product molecules to verify assignments and to provide information on their ground-state properties.[10] The B3LYP functional, 6-311+G(3d) basis set for nitrogen, and Los Alamos ECP plus DZ basis set for ruthenium and osmium were used in all calculations.[11−13] The calculated geometries, relative energies, and calculated frequencies are given in Tables 5 and 6, respectively.

10.1021/jp993338s CCC: $19.00 
Published on Web 01/25/2000

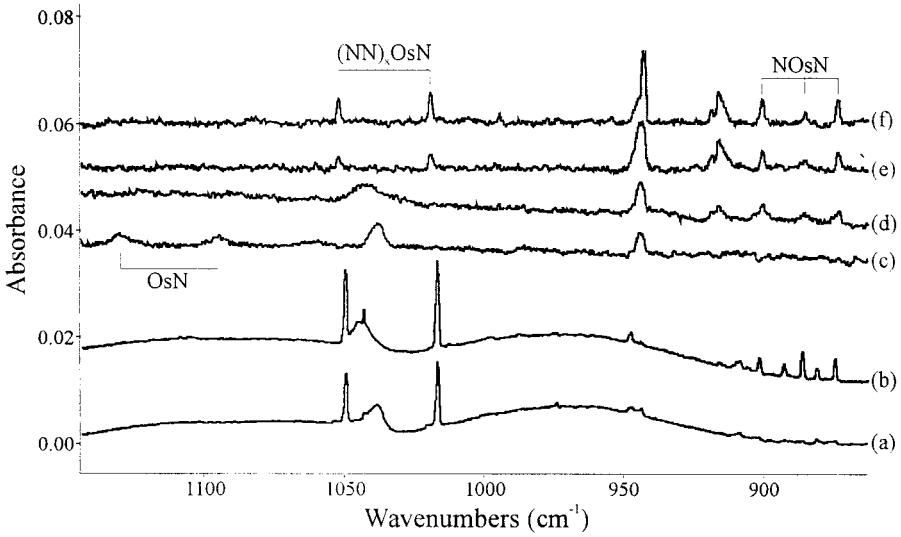


**Figure 1.** Infrared spectra in the 1140−860 $cm^{-1}$ region for laser-ablated osmium atoms co-deposited with nitrogen: (a) after 1 h deposition with pure $^{14}N_2 + {}^{15}N_2$ (43% + 57% mixture), (b) after annealing to 25 K with pure $^{14}N_2 + {}^{15}N_2$ (43% + 57% mixture), (c) after 1 h deposition with 2% $^{14}N_2$ + 2% $^{15}N_2$ in argon, (d) after annealing to 25 K, (e) after annealing to 40 K, (f) after annealing to 45 K. The 943 $cm^{-1}$ band that grows on annealing is probably due to $(N_2)_xOsO_2$.

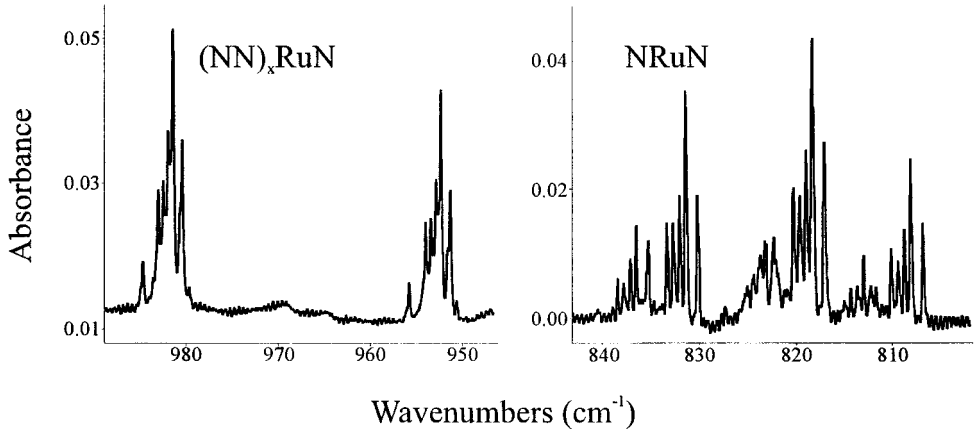


**Figure 2.** Infrared spectra in the 1000−950 $cm^{-1}$ and 840−800 $cm^{-1}$ regions with 0.125 $cm^{-1}$ resolution for laser-ablated ruthenium atoms co-deposited with $^{14}N_2 + {}^{15}N_2$ after annealing to 25 K.

**OsN and RuN.** A sharp, intense band observed at 1049.6 $cm^{-1}$ on deposition of osmium with pure nitrogen grows on early annealing but decreases markedly on photolysis (not shown). The $^{15}N_2$ counterpart for this band at 1016.6 $cm^{-1}$ defines an isotopic ratio of 1.03246, in close agreement with the harmonic diatomic ratio of 1.03247, calculated using the average atomic mass of osmium. No new bands are observed when osmium is deposited with an equal $^{14}N_2 + {}^{15}N_2$ mixture, indicating that only one nitrogen atom participates in the vibrational mode (Figure 1). These bands are due to dinitrogen complexed OsN in a nitrogen matrix. In argon, a weak band is observed at 1130.3 $cm^{-1}$, with a $^{15}N_2$ counterpart at 1094.8 $cm^{-1}$ that is present initially but disappears on annealing. A second band grows in at 1052.2 $cm^{-1}$ with a $^{15}N_2$ counterpart at 1019.2 $cm^{-1}$. Both bands have diatomic ratios, and are assigned to isolated and complexed OsN, respectively.

When ruthenium atoms are deposited with pure nitrogen, a group of bands is observed in the range 984.8−980.5 $cm^{-1}$, the most intense band being 981.5 $cm^{-1}$ (not shown). These bands are present on deposition, grow during early annealing, and decrease on photolysis, and are due to seven isotopes of ruthenium in natural abundance. The relative intensities of the bands is exactly what is expected for a mode involving only one ruthenium atom. The calculated ratios for each pair of frequencies are in excellent agreement with the ratios predicted for harmonic RuN, all being within 0.1% of those values. When ruthenium atoms are deposited with $^{15}N_2$, an analogous set of bands is observed in the range 955.8−951.3 $cm^{-1}$. Figure 2a shows the spectrum for the mixed $^{14}N_2 + {}^{15}N_2$ sample containing both features and no intermediate bands. The nitrogen isotopic ratios for different combinations of ruthenium isotopes have been calculated and compared to the corresponding values expected for the harmonic diatomic molecule RuN calculated using the appropriate masses, and all are found to agree within 0.1%. No intermediate bands are observed when a $^{14}N_2 + {}^{15}N_2$ mixture is used, indicating the participation of only one nitrogen atom, and these bands are assigned to the diatomic molecule RuN.

Analogous bands due to $Ru^{14}N$ and $Ru^{15}N$ are observed at 984.0 and 954.8 $cm^{-1}$ in argon matrixes. These are almost identical to the frequencies in solid nitrogen but are broad and no isotopic structure can be resolved. These bands are not present initially but grow in during annealing. Both OsN and RuN have been studied in detail by Ram, et al. using Fourier transform emission spectroscopy and high level ab initio calculations, and are found to have $^2\Delta$ and $^2\Sigma^+$ ground states, with the spectroscopic constants $r_o = 1.618$ Å, $\omega_e = 1148.0$ $cm^{-1}$, $\omega_e x_e = 5.5$ $cm^{-1}$ (OsN) and $r_o = 1.574$ Å, $\omega_e = 1122.0$

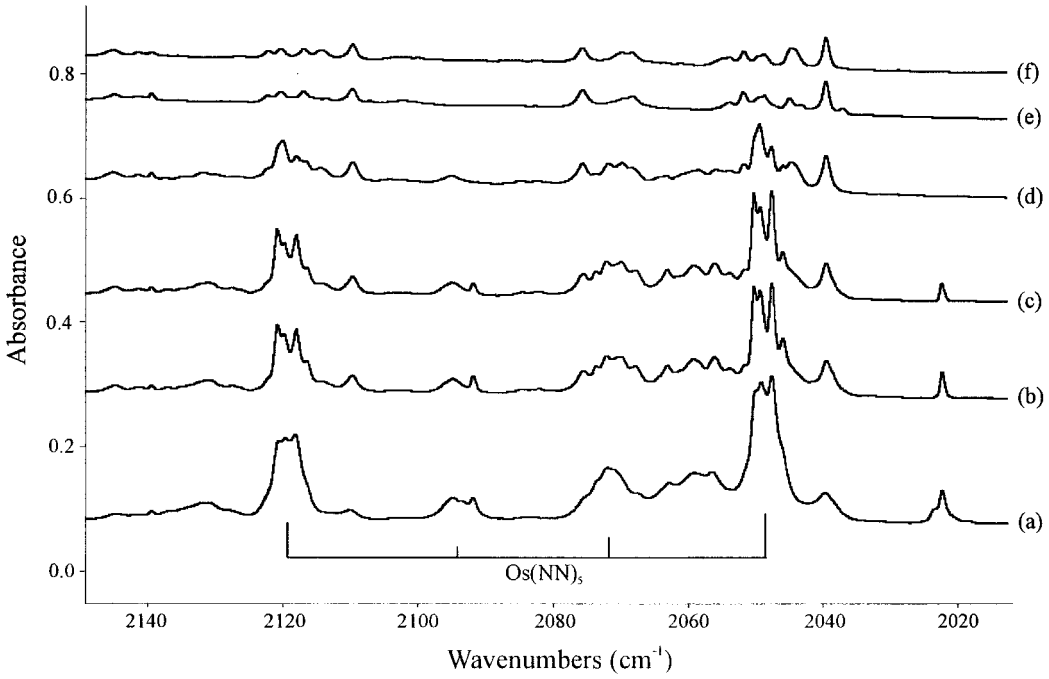


**Figure 3.** Infrared spectra in the 2150−2010 $cm^{-1}$ region for laser-ablated osmium atoms co-deposited with pure $^{14}N_2 + {}^{15}N_2$: (a) after 20 min deposition, (b) after annealing to 25 K, (c) after annealing to 30 K, (d) after annealing to 35 K, (e) after 25 min photolysis, (f) after annealing to 37 K.

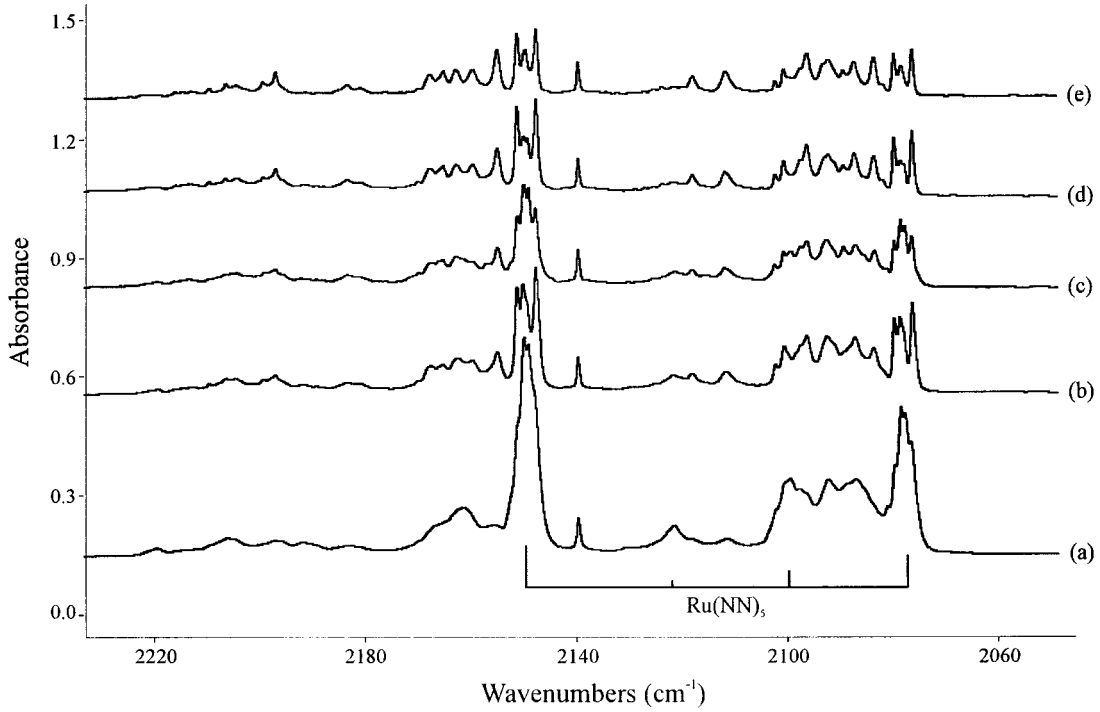


**Figure 4.** Infrared spectra in the 2230−2050 $cm^{-1}$ region for laser-ablated ruthenium atoms co-deposited with pure $^{14}N_2 + {}^{15}N_2$: (a) after 30 min deposition, (b) after annealing to 25 K, (c) after 30 min photolysis, (d) after annealing to 30 K, (e) after annealing to 35 K.

$cm^{-1}$, $\omega_e x_e = 6.5$ $cm^{-1}$ (RuN).[14,15] The gas-phase vibrational frequencies are much higher than the matrix values, and this is attributed to complexation of OsN and RuN by dinitrogen, to give $(NN)_xOsN$ and $(NN)_xRuN$. Only bands due to the most complexed form of the molecule are expected in a nitrogen matrix where the molecules are surrounded by nitrogen molecules, but additional absorptions may be observable in argon due to the uncomplexed and partially complexed molecules. This is the case for the osmium system, the 1130.3 $cm^{-1}$ band being only 7 $cm^{-1}$ below the (anharmonic) gas-phase frequency for OsN. The isolated OsN absorptions disappear on annealing and bands corresponding to the fully complexed molecule grow in, which are very close to the nitrogen matrix values, as has been observed in several metal nitride systems.[16−19] Vibrations due to the ligands should also be observable, but unfortunately the 2200−2300 $cm^{-1}$ region where dinitrogen ligands are expected is congested and no assignment can be made.

The results of the DFT calculations for the doublet states of these molecules are summarized in Tables 5 and 6. In both cases the initial calculations did not give the lowest energy states,

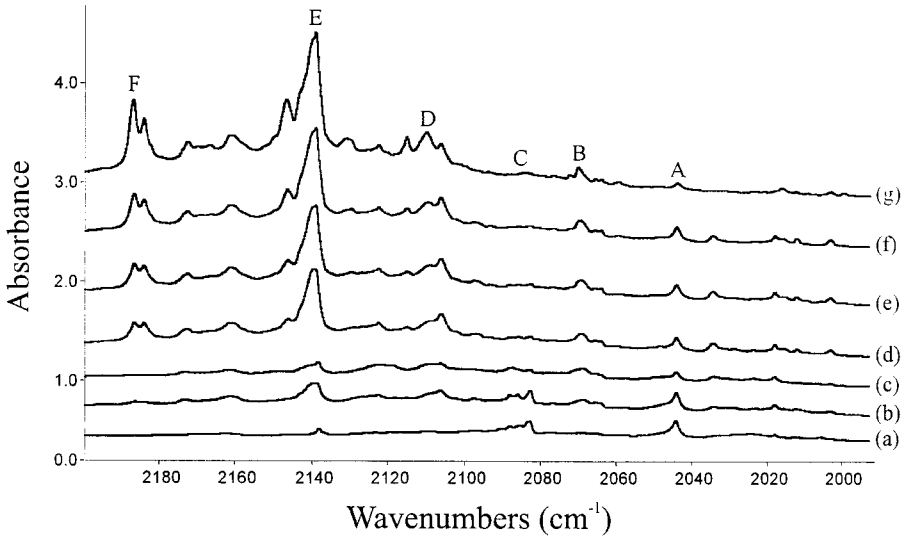


**Figure 5.** Infrared spectra in the 2200−2000 $cm^{-1}$ region for laser-ablated osmium atoms co-deposited with 3% $^{14}N_2$ in argon: (a) after 2 h deposition, (b) after annealing to 25 K, (c) after 25 min photolysis, (d) after annealing to 30 K, (e) after annealing to 35 K, (f) after annealing to 40 K, (g) after annealing to 45 K.

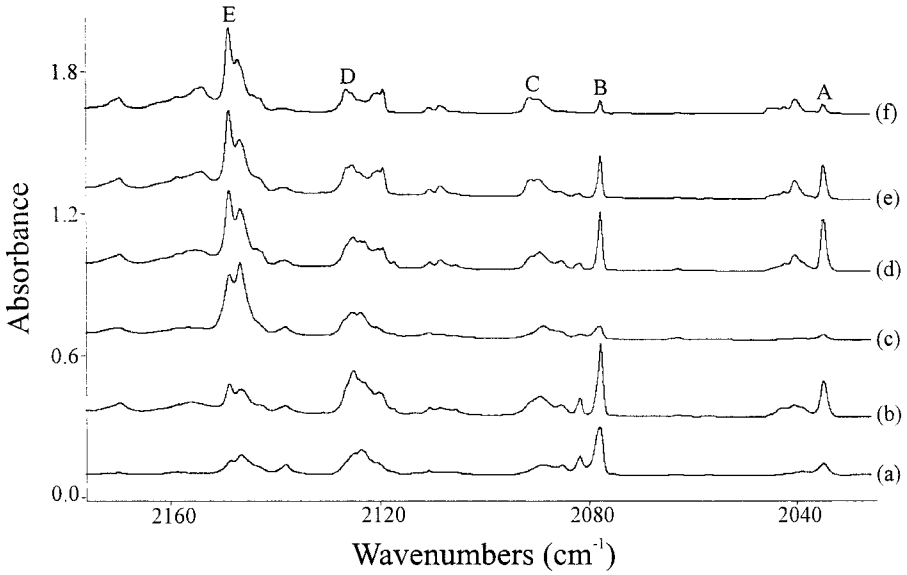


**Figure 6.** Infrared spectra in the 2170−2030 $cm^{-1}$ region for laser-ablated ruthenium atoms co-deposited with 4% $^{14}N_2$ in argon: (a) after 1 h deposition, (b) after annealing to 25 K, (c) after 30 min photolysis, (d) after annealing to 30 K, (e) after annealing to 35 K, (f) after annealing to 40 K.

**TABLE 1: Infrared Absorptions ($cm^{-1}$) Observed Following the Co-deposition of Laser-Ablated Osmium Atoms with Nitrogen at 7−8 K**

| $^{14}N_2$ | $^{15}N_2$ | $^{14}N_2 + {}^{15}N_2$ | isotopic ratio | assignment |
|---|---|---|---|---|
| 2119.7 | 2049.1 | 2119.7, 2093.5, 2071.8, 2059.1, 2049.1 | 1.03445 | $Os(NN)_5$ (site) |
| 2118.2 | 2047.6 | 2118.2, 2091.8, 2071.8, 2056.4, 2047.6 | 1.03448 | $Os(NN)_5$ |
| 2109.9 | 2039.4 | 2109.4, 2039.4 | 1.03457 | $Os(NN)_x$ (X<4) |
| 2091.8 | 2022.1 | 2091.8, 2022.1 | 1.03447 | $Os(NN)_x$ (X<4) |
| 1061.2 | 1028.2 | 1061.2, 1028.2 | 1.03209 | OsN (site) |
| 1049.6 | 1016.6 | 1049.6, 1016.6 | 1.03246 | OsN |
| 908.5 | 880.6 | 908.5, 892.4, 880.6 | 1.03168 | NOsN (site) |
| 903.4 | 875.7 | 903.4, 887.4, 875.5 | 1.03163 | NOsN (site) |
| 901.1 | 874.1 | 901.1, 885.5, 874.1 | 1.03089 | NOsN |
| 521.1 | 505.5 | 521.1, 513.7, 505.5 | 1.03086 | $Os(NN)_5$ (site) |
| 518.2 | 502.5 | 518.2, 511.1, 502.5 | 1.03124 | $Os(NN)_5$ |

and different initial orbital occupations were used in subsequent calculations to find the ground states for OsN and RuN which DFT predicts to be $^2\Delta$ and $^2\Sigma^+$, respectively, in agreement with experiment.[14,15] The calculated bond lengths of 1.621 and 1.581 Å are also in excellent agreement with the experimental values, being too long by only 0.003 and 0.007 Å, respectively. The calculated harmonic frequencies are higher than the gas-phase values, and must be scaled by 0.942 and 0.945, which are

**TABLE 2: Infrared Absorptions ($cm^{-1}$) Observed following the Co-deposition of Laser-Ablated Osmium Atoms with Nitrogen/Argon Mixtures at 7−8 K**

| $^{14}N_2$ | $^{15}N_2$ | $^{14}N_2 + {}^{15}N_2$ | isotopic ratio | assignment |
|---|---|---|---|---|
| 2186.8 | *a* | *a* | | |
| 2138.9 | 2067.6 | 2138.9, 2067.6[a] | 1.03448 | $Os(NN)_5$ |
| 2106.0 | *a* | *a* | | $Os(NN)_4$ |
| 2083.2 | 2013.9 | 2083.1, 2033.8, 2013.9 | 1.03441 | $Os(NN)_2$ |
| 2070.0 | *a* | *a* | | $Os(NN)_3$ |
| 2044.2 | 1976.2 | 2044.2, 1976.2 | 1.03441 | Os(NN) |
| 1130.3 | 1094.8 | 1130.3, 1094.8 | 1.03243 | OsN |
| 1052.2 | 1019.2 | 1052.2, 1019.2 | 1.03238 | $(NN)_xOsN$ |
| 900.4 | 872.9 | 900.4, 884.7, 872.9 | 1.03150 | NOsN |

[a] Spectra were too congested to observe these bands.

reasonable scale factors for the B3LYP functional, basis set, and ECP used.[20] It is clear from these results that DFT reproduces the experimental results very effectively. The calculated parameters for two higher lying doublet states of OsN and RuN are also included in Tables 5 and 6 which are in reasonable agreement with those calculated using high level ab initio methods.[14,15]

It is interesting to compare the force constants for OsN, RuN, and FeN, which are shown in Table 7. These were calculated using the matrix frequencies for the complexed molecules $(NN)_xMN$ as discussed above. It is still valid to calculate the complexed MN force constant using the equation for a harmonic diatomic molecule provided that the mechanical coupling between the MN group and the rest of the molecule is weak. This is found to be the case for OsN where the isotopic ratios are almost identical for isolated OsN in argon (1.03243) and fully complexed OsN in nitrogen (1.03246), both being close to the harmonic diatomic value of 1.03247. This is also apparent from the lack of a secondary isotopic effect for the bands due to $(NN)_xOsN$ and $(NN)_xRuN$ in pure nitrogen matrixes. Thus, changes in frequencies as the molecules are complexed by dinitrogen are due to an electronic effect and not a mechanical effect. The force constant is lowest for FeN, increasing by ∼21% moving down each row in the periodic table. The increase in bond strength moving down the group is consistent with the fact that 5d metals form stronger bonds than the 3d or 4d metals in the same group with hydrides, phosphines, and other ligands.[21] The force constants for $^{192}OsN$ and $^{102}RuN$ have also been calculated using the gas-phase harmonic frequencies, and are included in Table 7. These are larger than the matrix values, which means that the M−N bond is significantly weakened when additional $N_2$ molecules bind to the metal center. No experimental data is available for isolated FeN, only complexed FeN was observed in the previous matrix isolation study of the iron nitrides. On the basis of the osmium and ruthenium results, a decrease of 20−30% would be expected in the force constant for $(N_2)_xFeN$ relative to FeN.

**NOsN and NRuN.** When osmium atoms are deposited with pure nitrogen, a weak band is observed at 901.2 $cm^{-1}$ that grows in strongly on annealing and is diminished on photolysis (not shown). A less intense matrix site at 908.3 $cm^{-1}$ is diminished on annealing but grows in on photolysis. The $^{15}N_2$ counterparts for these bands are at 880.4 and 873.8 $cm^{-1}$, respectively, and give almost identical isotopic ratios of 1.03136 and 1.03169 for the different matrix sites. These are lower than the diatomic value of 1.03216 indicating a greater participation of the metal atom in the mode relative to the diatomic molecule. When the experiment is repeated using a $^{14}N_2 + {}^{15}N_2$ mixture, an intermediate band is observed at 885.6 $cm^{-1}$ with a weaker matrix site at 892.2 $cm^{-1}$, which are more intense than either of the pure isotope bands (Figure 1a). The intensity pattern for this triplet of peaks is appropriate for a vibrational mode that involves two equivalent nitrogen atoms, and NOsN is the most logical assignment for these bands. The fact that the intermediate band is observed shows that the molecule is formed through reaction 1, rather than reaction 2, since no isotopically scrambled $^{14}N^{15}N$ is present to form $^{14}NOs^{15}N$ by direct insertion. This is reasonable considering the abundance of OsN and nitrogen atoms in the pure nitrogen matrix, the latter being evident from

**TABLE 3: Infrared Absorptions ($cm^{-1}$) Observed following the Co-deposition of Laser-Ablated Ruthenium Atoms with Nitrogen at 7−8 K**

| $^{14}N_2$ | $^{15}N_2$ | $^{14}N_2 + {}^{15}N_2$ | isotopic ratio | assignment |
|---|---|---|---|---|
| 2151.2 | 2079.6 | 2150.0, 2121.6, 2099.5, 2087.0, 2078.4 | 1.03443 | $Ru(NN)_5$ site |
| 2149.3 | 2077.6 | | 1.03451 | $Ru(NN)_5$ |
| 2147.5 | 2076.1 | | 1.03439 | $Ru(NN)_5$ site |
| 2147.0 | 2075.5 | | 1.03445 | $Ru(NN)_5$ site |
| 2003.0 | 1937.2 | 2003.0, 1992.9, 1948.8, 1937.2 | 1.03397 | $N_3^-$ |
| 1932.2 | 1868.1 | *a* | 1.03431 | |
| 1874.9 | 1841.8 | 1874.9, 1841.8 | 1.01797 | NO |
| 1657.7 | 1603.3 | 1657.7, 1649.4, 1613.0, 1603.3 | 1.03393 | $N_3$ |
| 984.8 | 955.8 | 984.8, 955.8 | 1.03034 | $^{96}RuN$ |
| 983.6 | *b* | 983.6, *b* | | $^{98}RuN$ |
| 983.1 | 954.0 | 983.1, 954.0 | 1.03050 | $^{99}RuN$ |
| 982.5 | 953.4 | 982.5, 953.4 | 1.03052 | $^{100}RuN$ |
| 982.0 | 952.9 | 982.0, 952.9 | 1.03054 | $^{101}RuN$ |
| 981.5 | 952.4 | 981.5, 952.4 | 1.03055 | $^{102}RuN$ |
| 980.5 | 951.3 | 980.5, 951.3 | 1.03069 | $^{104}RuN$ |
| 838.4 | *b* | 838.4, *b* | | $N^{99}RuN$ (site) |
| 837.8 | *b* | 837.8, *b* | | $N^{100}RuN$ (site) |
| 837.1 | *b* | 837.1, *b* | | $N^{101}RuN$ (site) |
| 836.5 | *b* | 836.5, *b* | | $N^{102}RuN$ (site) |
| 835.3 | *b* | 835.3, *b* | | $N^{104}RuN$ (site) |
| 833.4 | 810.1 | 833.4, 820.3, 810.1 | 1.02876 | $N^{99}RuN$ |
| 832.7 | 809.4 | 832.7, 819.6, 809.4 | 1.02879 | $N^{100}RuN$ |
| 832.1 | 808.7 | 832.1, 819.0, 808.7 | 1.02894 | $N^{101}RuN$ |
| 831.5 | 808.1 | 831.5, 818.3, 808.1 | 1.02896 | $N^{102}RuN$ |
| 830.2 | 806.8 | 830.2, 817.1, 806.8 | 1.02900 | $N^{104}RuN$ |
| 499.0 | 486.2 | 499.0, 493.4, 486.2 | 1.02633 | $Ru(NN)_5$ |

[a] Spectra were too congested to observe these bands. [b] Bands could not be resolved.

**TABLE 4: Infrared Absorptions ($cm^{-1}$) Observed following the Co-deposition of Laser-Ablated Ruthenium Atoms with Nitrogen/Argon at 7−8 K**

| $^{14}N_2$ | $^{15}N_2$ | $^{14}N_2 + {}^{15}N_2$ | isotopic ratio | assignment |
|---|---|---|---|---|
| 2148.8 | 2077.3 | *a* | 1.03442 | $Ru(NN)_5$ |
| 2126.5 | 2055.7 | *a* | 1.03444 | $Ru(NN)_4$ |
| 2119.3 | 2048.8 | *a* | 1.03441 | $Ru(NN)_4$ (site) |
| 2091.2 | 2021.5 | *a* | 1.03448 | $Ru(NN)_3$ |
| 2077.6 | 2008.6 | *a* | 1.03435 | $Ru(NN)_2$ |
| 2034.6 | 1967.1 | 2034.6, 1967.1 | 1.03431 | Ru(NN) |
| 984.0 | 954.8 | 984.0, 954.8 | 1.03058 | RuN |
| 831.9 | 808.4 | 831.9, 818.7, 808.4 | 1.02907 | $N^{102}RuN$ |
| 830.5 | 807.1 | 830.5, 817.4, 807.1 | 1.02899 | $N^{104}RuN$ |

[a] Spectra were too congested to observe these bands.

the band at 1657.4 $cm^{-1}$ due to $N_3$.[16,22]

$$OsN + N \rightarrow NOsN \quad (1)$$

$$Os + N_2 \rightarrow NOsN \quad (2)$$

Analogous bands are observed at 900.3, 884.7, and 872.9 $cm^{-1}$ when osmium is co-deposited with $^{14}N_2 + {}^{15}N_2$ in argon, very close to the pure nitrogen values (as was found for OsN). However, the annealing behavior for these bands in argon is different from that in pure nitrogen (Figure 1). The bands are not present initially, but grow in during annealing. The intermediate band also grows in, but not to the same extent, and after the final annealing cycle the intensity ratio is approximately 3:1:3. This implies that reaction 2 is dominant, but that reaction 1 also occurrs to a small extent. These observations demonstrate that osmium atoms insert into the dinitrogen molecule and break the strong triple bond in a cold argon matrix. This is a significant result, as it shows that the reaction *does not require activation energy and is thermodynamically favorable*. Since the temperature in the matrix is low, the entropy contribution to the free energy change is negligible compared to the enthalpy change. Given that the bond enthalpy in $N_2$ is 945 kJ/mol,[23] the average Os−N bond enthalpy in NOsN must be ≥473 kJ/mol. The high affinity of osmium for dinitrogen shown here parallels the high activity of the metal as a catalyst in ammonia synthesis.[6] It could be argued that osmium reacts with dinitrogen in two steps, rather than a direct insertion. The first step would be to form OsN and N, which would then combine to give NOsN. If the OsN and N were effectively trapped together in the argon cage then little $^{14}NOs^{15}N$ would be expected in the mixed experiment using $^{14}N_2 + {}^{15}N_2$. However, for the first step to be thermodynamically favorable, the OsN bond strength would have to exceed the $N_2$ bond strength, and this is not expected to be the case as is discussed below. This reaction can occur on deposition with energetic metal atoms, but not on annealing with cold metal atoms.

The growth of NOsN on annealing in solid argon and the near agreement of NOsN frequencies in solid argon and nitrogen suggests that the NOsN molecule may be ligated by dinitrogen but to a lesser degree than $(NN)_xOsN$ in dinitrogen. However, dinitrogen ligation of the NOsN insertion product may provide thermodynamic assistance for the insertion reaction 2.

The 14/15 isotopic ratios of 1.03136 and 1.03115 for these bands in $N_2$ and $N_2$/Ar can be used in conjunction with the appropriate **G** matrix elements to estimate the bond angle for the bent symmetrical molecule.[24,25] If the observed bands are

**TABLE 5: Calculated States, Geometries, and Relative Energies for Osmium Nitride Species**

| molecule | state | energy (kJ/mol) | $\langle S^2 \rangle$ | geometry (Å, deg) | frequencies ($cm^{-1}$) [intensities (km/mol)] |
|---|---|---|---|---|---|
| OsN | $^2\Delta$ | 0 | 0.7503 | *r*(Os−N): 1.6208 | 1219.1 [39] |
| | $^2\Sigma^+$ | +70 | 0.7500 | *r*(Os−N): 1.6123 | 1230.0 [36] |
| | $^2\Pi$ | +160 | 0.7755 | *r*(Os−N): 1.6797 | 1036.3 [28] |
| NOsN | $^1A_1$ | +110 | | *r*(Os−N): 1.6825, ∠NOsN: 105.1° | 1121.6 [6], 1005.0 [39], 457.5 [0] |
| | $^3B_1$ | +184 | 2.0000 | *r*(Os−N): 1.7000 ∠NOsN: 111.8° | 1053.8 [4], 891.6 [109], 396.1 [0] |
| | $^5A_2$ | +244 | 6.0001 | *r*(Os−N): 1.7305, ∠NOsN: 123.5° | 977.2 [27], 567.3 [2], 269.5 [2] |
| NOsOsN | $^1A$ | −205[a] | | *r*(Os−N): 1.639 *r*(Os−Os): 2.412 ∠NOsOs: 103.1° $\phi$(NOsOsN): 109.6° | 1172.7 [95], 1159.4 [7], 243.3 [4], 198.4 [0], 167.6 [17], 136.0 [3] |

[a] Relative to twice the energy of OsN ($^2\Delta$).

**TABLE 6: Calculated States, Geometries, and Relative Energies for Ruthenium Nitride Species**

| molecule | state | energy (kJ/mol) | $\langle S^2 \rangle$ | geometry (Å, deg) | frequencies ($cm^{-1}$) [intensities (km/mol)] |
|---|---|---|---|---|---|
| RuN | $^2\Sigma^+$ | 0 | 0.7500 | *r*(Ru−N): 1.5810 | 1187.4 [150] |
| | $^2\Pi$ | +62 | 0.7557 | *r*(Ru−N): 1.6386 | 1028.3 [29] |
| | $^2\Delta$ | +76 | 0.7519 | *r*(Ru−N): 1.6280 | 1024.8 [156] |
| NRuN | $^1A_1$ | +364 | | *r*(Ru−N): 1.6864, ∠NRuN: 107.2° | 1041.2 [10], 856.0 [100], 409.2 [6] |
| | $^3B_1$ | +351 | 2.0002 | *r*(Ru−N): 1.687 ∠NRuN: 113.0° | 927.0 [7], 897.2 [4], 261.1 [0] |
| | $^5A_1$ | +396 | 6.0005 | *r*(Ru−N): 1.724, ∠NRuN: 116.5° | 984.7 [42], 378.2 [5], 249.2 [15] |
| $Ru_2N_2$ | $^3B_2$ | −234[a] | 2.0004 | *r*(Ru−N): 1.812 *r*(Ru−Ru): 2.746 ∠RuNRu: 98.5° $\phi$(NRuRuN): 155.6° | 807.7 [15], 780.4 [4], 597.7 [88], 481.6 [0], 362.3 [12], 235.3 [34] |

[a] Relative to twice the energy of RuN ($^2\Sigma^+$).

**TABLE 7: Calculated Force Constants ($nm^{-1}$) for MN, $(N_2)_xMN$, and NMN (M = Fe, Ru, Os)**

| | | NMN | |
|---|---|---|---|
| metal | MN $f_{M-N}$ | $f_{M-N}$ | $f_{M-N/M-N}$ |
| iron | 575 | 554 | 58 |
| ruthenium | 702 (913)[a] | 588 | 115 |
| osmium | 851 (1013)[b] | 722 | 115 |

[a] Force constant calculated using the gas-phase data in ref 14. [b] Force constant calculated using the gas-phase data in ref 15.

due to the $\nu_3$ mode then upper limit estimates of 120° and 126° are derived for NOsN in nitrogen and argon matrixes, respectively. This is consistent with the large number of NMN molecules characterized, which have similar angles.[7,16−19] The bent geometries for most of these molecules agree with the predictions of a Walsh-like treatment of $AB_2$ triatomics where the central atom is a transition metal, and molecules with less than 19 valence electrons are bent.[26] The isotopic ratio for the terminal atoms in the $\nu_3$ mode of a triatomic molecule gives an upper limit on the bond angle.[24,25] The isotopic ratio for the central atom would give a lower limit on the angle, but unfortunately the osmium isotopes in NOsN could not be resolved. The bands in the nitrogen matrix are sharper and their positions measured with greater accuracy, so the angle calculated using these numbers is considered to be more reliable. Considering the results for iron and ruthenium (see below), the best estimate for the NOsN bond angle is 115 ± 5°.

When ruthenium is co-deposited with pure $^{14}N_2$, a group of five bands is observed in the range 833.4−830.2 $cm^{-1}$ with the same characteristic intensity pattern observed for RuN, indicating that only one ruthenium atom is involved in the mode. These bands correspond to the five heaviest isotopes of ruthenium, the bands due to other isotopes not being observed. Weaker matrix sites to these bands are observed in the range 838.4−835.3 $cm^{-1}$, analogous to the higher frequency matrix site observed for NOsN. The $^{15}N$ counterparts for the dominant matrix site are in the range 810.1−806.8 $cm^{-1}$, and when the experiment is repeated with a $^{14}N_2 + {}^{15}N_2$ mixture intermediate bands are observed in the range 820.3−817.1 $cm^{-1}$ to give an overall intensity pattern that is appropriate for a mode that involves two equivalent nitrogen atoms. The most straightforward assignment for these bands is to NRuN, formed by the addition of nitrogen atoms to RuN molecules. Unlike NOsN, both metal and nitrogen isotopic data are available to estimate both lower and upper limits for the bond angle, respectively.[24,25] Using of all the available isotopic data allows upper and lower limits of 117° and 109° to be determined for the N−Ru−N bond angle. The average value of 113° represents a reliable estimate of the bond angle owing to cancellation of anharmonic effects.

Bands due to NRuN are observed in argon matrixes at 831.9/830.5, 818.7/817.4, and 808.4/807.1 $cm^{-1}$ where bands due to the $^{104}Ru$ and $^{102}Ru$ isotopes can be resolved. However these bands are weak and broad, and the greater uncertainty in their positions would lead to an inferior bond angle estimate compared to the nitrogen matrix data where the bands were sharp and intense. On annealing the argon matrix, the bands due to $^{14}NRu^{14}N$, $^{15}NRu^{15}N$, and $^{14}NRu^{15}N$ grow slightly but the same proportion, indicating that the molecule is being formed by the addition of a nitrogen atom to RuN rather than the direct insertion of ruthenium into a dinitrogen molecule.

The iron dinitride NFeN was observed previously in this laboratory and the bond angle was calculated to be 115 ± 5° using nitrogen and iron isotopic data, which gave upper and lower limits of 121° and 110°, respectively, very similar to the values for NRuN and NOsN. There is enough isotopic data available to calculate the force constants for these molecules, using the best estimates for the bond angles and the appropriate atomic masses to calculate the **G** matrix elements,[28] and the results are shown in Table 7. All resolvable bands due to the different isotopes for iron and ruthenium in solid nitrogen were used, and stated force constants are averages over two (NFeN) and five (NRuN) values calculated using different isotopes. The metal isotopes for osmium could not be resolved and the average atomic mass for osmium was used. Considering also the uncertainty in the bond angle, the force constants are expected to be in greatest error for NOsN. The force constants are less than those for the corresponding diatomic molecules but show the same trend, increasing down the metal group.

These force constants may be used in conjunction with the spectroscopic parameters derived previously for OsN and RuN[14,15] to estimate bond energies. The $\omega_e$ and $\omega_e x_e$ values for a diatomic molecule can be used to estimate $D_e$ analytically if a Morse potential is assumed.[29] In this way, values of 722 and 579 kJ/mol are estimated for $D_e$(OsN) and $D_e$(RuN). The force constant calculated for NOsN is 15.2% lower than that for OsN, and if it is assumed that the bond energies scale the same way, the bond dissociation energy in NOsN is estimated to be 613 kJ/mol, well above the lower limit of 473 kJ/mol predicted earlier. The force constants for OsN and NOsN in nitrogen, where both are complexed by dinitrogen, were used in making the comparison, since there is no force constant for NOsN with which to compare that for OsN in the gas phase. If the force constant treatment is applied to the ruthenium data, a bond dissociation energy of 485 kJ/mol is estimated for each bond in NRuN. This upper limit is only slightly above the lower limit of ∼473 kJ/mol required for a spontaneous insertion reaction, and so direct insertion by ruthenium into the dinitrogen bond is not likely on annealing. It is clear from this discussion that the Os−N bond energy in NOsN is well above the lower limit of ∼473 kJ/mol required for the insertion of osmium into the dinitrogen bond to be thermodynamically favorable. The Ru−N bond energy in NRuN is estimated to be much closer to this lower limit, and the available experimental data indicates that it is too low to provide a driving force for the spontaneous insertion by ruthenium into the dinitrogen bond.

The results of the DFT calculations for the triatomics are given in Tables 6 and 7. NOsN is found to have an $^1A_1$ ground state with a bond angle of 105.1°, in reasonable agreement with the estimated experimental value. The calculated $\nu_3$ frequency is significantly lower than the $\nu_1$ frequency, and has a much higher intensity. This is in agreement with experiment where the $\nu_1$ mode could not be observed, and the intermediate band in the mixed isotopic experiment is red shifted from the midpoint of the pure isotope bands. The $\nu_3$ frequency is higher than the experimental value, and a scale factor of 0.897 is required, which is reasonable for the density functional and basis set used.[17] The results for NRuN are more ambiguous. The $^3B_1$ state is lowest in energy, and the bond angle of 113.0° is in excellent agreement with the value of 112.8° calculated from the isotopic data. However, a large negative frequency is calculated for this state and so it must be rejected. The triplet states $^3A_1$, $^3A_2$, and $^3B_2$ were calculated by altering the MO occupations, but these are all more than 65 kJ/mol higher in energy than the $^3B_1$ state. The $^1A_1$ state for NRuN is only 13 kJ/mol higher than the $^3B_1$ state, and the calculated geometry is in reasonable agreement with the experimental value. The calculated frequencies for this state are also reasonable, the $\nu_3$ mode has a much higher

**TABLE 8: NBO Bonding Analysis for Osmium and Ruthenium Nitride Products**

| molecule | bond | population[a] | %M[b] | %ns[c] | %np[c] | %(n−1)d[c] | %N[b] | %2s[c] | %2p[c] |
|---|---|---|---|---|---|---|---|---|---|
| OsN ($^2\Delta$) α | Os−N ($\pi$) | 1.00 (0.00) | 52.9 | 0.0 | 0.0 | 100.0 | 47.1 | 0.0 | 99.3 |
| Os−N ($\pi$) | 1.00 (0.00) | 52.9 | 0.0 | 0.0 | 100.0 | 47.1 | 0.0 | 99.3 | |
| Os−N ($\sigma$) | 1.00 (0.01) | 43.5 | 36.5 | 0.6 | 62.9 | 56.5 | 17.4 | 82.2 | |
| OsN ($^2\Delta$) $\beta$ | Os−N ($\sigma$) | 1.00 (0.01) | 42.3 | 30.2 | 0.6 | 69.2 | 57.7 | 17.6 | 81.9 |
| Os−N ($\pi$) | 1.00 (0.00) | 44.3 | 0.0 | 0.0 | 100.0 | 55.7 | 0.0 | 99.4 | |
| Os−N ($\pi$) | 1.00 (0.00) | 44.3 | 0.0 | 0.0 | 100.0 | 55.7 | 0.0 | 99.4 | |
| NOsN ($^1A_1$) | Os−$N_1$ ("$\pi$") | 2.00 (0.00) | 58.3 | 0.0 | 0.0 | 100.0 | 41.7 | 0.0 | 100.0 |
| Os−$N_1$ ("$\sigma$") | 1.89 (0.16) | 36.0 | 33.1 | 3.2 | 63.7 | 64.0 | 17.7 | 81.8 | |
| Os−$N_1$ ("$\sigma+\pi$") | 1.69 (0.27) | 33.9 | 1.9 | 12.3 | 85.8 | 66.1 | 0.1 | 99.2 | |
| Os−$N_2$ ("$\pi$") | 2.00 (0.00) | 58.3 | 0.0 | 0.0 | 100.0 | 41.7 | 0.0 | 100.0 | |
| Os−$N_2$ ("$\sigma$") | 1.89 (0.16) | 36.0 | 33.1 | 3.2 | 63.7 | 64.0 | 17.7 | 81.8 | |
| Os−$N_2$ ("$\sigma+\pi$") | 1.69 (0.27) | 33.9 | 1.9 | 12.3 | 85.8 | 66.1 | 0.1 | 99.2 | |
| RuN ($^2\Sigma^+$) α | Ru−N ($\pi$) | 1.00 (0.00) | 50.3 | 0.0 | 0.0 | 100.0 | 49.7 | 0.0 | 99.5 |
| Ru−N ($\pi$) | 1.00 (0.00) | 50.3 | 0.0 | 0.0 | 100.0 | 49.7 | 0.0 | 99.5 | |
| Ru−N ($\sigma$) | 1.00 (0.02) | 41.1 | 43.3 | 0.7 | 56.0 | 58.9 | 17.1 | 82.7 | |
| RuN ($^2\Sigma^+$) $\beta$ | Ru−N ($\sigma$) | 1.00 (0.02) | 50.8 | 1.3 | 0.1 | 98.6 | 49.2 | 10.2 | 89.3 |
| Ru−N ($\pi$) | 1.00 (0.00) | 48.0 | 0.0 | 0.0 | 100.0 | 52.0 | 0.0 | 99.5 | |
| Ru−N ($\pi$) | 1.00 (0.00) | 48.0 | 0.0 | 0.0 | 100.0 | 52.0 | 0.0 | 99.5 | |
| NRuN ($^1A_1$) | Ru−$N_1$ ("$\pi$") | 2.00 (0.00) | 64.0 | 0.0 | 0.0 | 100.0 | 36.0 | 0.0 | 99.3 |
| Ru−$N_1$ ("$\sigma$") | 1.96 (0.26) | 41.4 | 31.7 | 0.4 | 67.9 | 58.6 | 14.5 | 85.1 | |
| Ru−$N_1$ ("$\sigma+\pi$") | 1.93 (0.51) | 47.2 | 11.1 | 0.2 | 88.7 | 52.8 | 0.1 | 99.5 | |
| Ru−$N_2$ ("$\pi$") | 2.00 (0.00) | 64.0 | 0.0 | 0.0 | 100.0 | 36.0 | 0.0 | 99.3 | |
| Ru−$N_2$ ("$\sigma$") | 1.92 (0.19) | 37.7 | 45.8 | 0.4 | 53.8 | 62.3 | 14.5 | 85.1 | |

[a] The number in parentheses is the population of the corresponding antibond. [b] The total contribution of the atom's orbitals to the bond. [c] Hybridization of the bond at the atom.

intensity and is lower in frequency than the $\nu_1$ mode. The calculated frequency is only slightly higher than the experimental value, and the scale factor for this mode is 0.97. This is much higher than that for NOsN which is unexpected but does not necessarily mean it is wrong, just that DFT is an approximate treatment. The lowest quintet state, $^5A_2$, is 45 kJ/mol higher than the $^3B_1$ state which is not unreasonably high, but must be rejected since the $\nu_3$ frequency and intensity is unrealistically low. In summary, the ground states of both NOsN and NRuN are found to be $^1A_1$, although further calculations on these molecules would be useful.

**$Os_2N_2$ and $Ru_2N_2$.** It could be argued that the bands assigned above to NOsN and NRuN are due to dimers of the diatomic molecules, since the observation of the scrambled isotopic molecule in the mixed $^{14}N_2 + {}^{15}N_2$ experiment would be consistent with the combination of two diatomic molecules. However, this assignment must be rejected in light of the annealing behavior of the bands in an argon matrix. If a dimer were formed via the combination of OsN molecules, then a 1:2:1 intensity pattern would be observed. There is no way to reconcile assignment of the observed bands to $(OsN)_2$ with the low intensity of the intermediate bands relative to the pure isotope bands in argon. The growth of the analogous bands in the ruthenium nitride system on annealing is consistent with the formation of $(RuN)_2$, but the ruthenium isotopic data clearly show that only one ruthenium atom is present.

Both cyclic and open structural isomers with the formulas $Os_2N_2$ and $Ru_2N_2$ have been calculated using DFT, and the lowest energy geometries for each metal are given in Tables 5 and 6. It is interesting that these molecules are not observed despite the abundance of diatomic molecules and the calculated energy changes for the dimerization reactions (−205 kJ/mol for OsN, −234 kJ/mol for RuN). This suggests that either the diatomic molecules are not very mobile or that the reaction is an activated process that cannot occur at such low temperatures. Low mobility of isolated species is unlikely to be the cause considering the number of aggregate species that are observed in so many other metal nitride and oxide systems. A significant activation energy would also be surprising since OsN and RuN have doublet ground states, ie they are both open shell species, and reactions between two open shell species do not usually require activation energy. The absence of dimerization reactions between the nitrides can be explained by the fact that these molecules are heavily ligated in argon and nitrogen matrixes, and the combination reaction would also involve a rearrangement of the surrounding dinitrogen ligands. The more tightly the ligands in these complexes are bound, the more hindered the combination reaction will be. The strength of the bonding in these complexes is of course unknown, but can be inferred from the red shift in metal nitride frequency when the isolated molecule is complexed by dinitrogen. For example, the yttrium and rhodium nitrides YN and RhN were only weakly complexed by dinitrogen, as shown by red shifts of only 29 and 29.7 $cm^{-1}$ between the isolated diatomic molecules in argon and their dinitrogen complexed forms.[18,30] By contrast, the Os−N frequency is red shifted by 78.1 $cm^{-1}$, and the tighter binding in this complex that this would suggest may be enough to completely hinder the dimerization reaction.

**Bonding Analyses.** The bonding in the diatomic and triatomic molecules has been examined using the Natural Bond Orbitals (NBO),[31] and the results are summarized in Table 8. Both OsN and RuN have triple bonds, consisting of one $\sigma$ and two $\pi$ bonds. However, the force constants calculated earlier show that the bond strengths are quite different despite having the same bond orders. NOsN is predicted to consist of two triple bonds, each formed from a sigma type bond, a pi type bond, and a third bond that is a mixture of $\sigma$ and $\pi$ components. NRuN is similar, except that there is only one sigma/pi mixed bond to shared between both bonds, to give a bond order of two and a half rather than three. The M−N bonds are not very polarized toward either atom and have no significant ionic character, in agreement with studies of other transition metal and lanthanide nitrides.[32,33]

**$Os(NN)_n$ and $Ru(NN)_n$.** When osmium is co-deposited with pure nitrogen, intense bands are observed at 2119.7 and 2118.2 $cm^{-1}$. These bands decrease slowly on annealing but are destroyed on photolysis. The $^{15}N_2$ counterparts are at 2049.1 and 2047.6 $cm^{-1}$, giving isotopic ratios of 1.03445, and 1.03448 which are typical of dinitrogen stretching modes. These are clearly due to an osmium dinitrogen complex in different matrix sites. When osmium is co-deposited with a $^{14}N_2 + {}^{15}N_2$ mixture,

weaker intermediate bands are observed at 2094.8/2091.8, 2071.8, and 2059.1/2056.4 $cm^{-1}$ (Figure 3). The presence of what appears to be three intermediate bands that are weaker than the pure isotope absorptions suggests that four dinitrogen units are bound to the metal in a tetrahedral geometry.[34] Weaker bands are observed in the range 2200−2125 $cm^{-1}$ that are probably due to the mixed isotope symmetric stretching modes, though specific assignments cannot be made with certainty. A much weaker band is observed at 518.2 $cm^{-1}$ that tracks with the high-frequency bands; the $^{15}N_2$ counterpart for this band at 502.5 $cm^{-1}$ gives an isotopic ratio of 1.03124, which is appropriate for an M−$N_2$ stretching mode of a dinitrogen complex. One intermediate band is observed in the mixed isotopic experiment at 511.1 $cm^{-1}$ to give a 1:2:1 intensity pattern. A better assignment for these bands is to $Os(N_2)_5$, which is expected to be the most highly coordinated osmium dinitrogen complex based on the previous matrix isolation study of the iron dinitrides, the known carbonyl chemistry of the iron group, and the 18 electron rule.[7,35−37] Two infrared active dinitrogen vibrations are expected for a trigonal bipyramidal five coordinate complex; the out of phase stretch of the axial ligands, $a_2''$, and the degenerate stretching mode of the equatorial ligands, e′. It is questionable whether the 2056.4 $cm^{-1}$ band is actually an intermediate component, and if this is ignored then the observed nonbinomial intensity pattern is consistent with the degenerate stretching mode of the equatorial ligands in a complex with $D_{3h}$ symmetry.[34] The second mode expected for this geometry is not observed, and this may be due to an interaction between the complex and the host matrix or an inherently low intensity. If this assignment is correct, then the 1:2:1 intensity pattern observed in the mixed isotopic experiment near 500 $cm^{-1}$ would be due to the out of phase Os−N stretching modes for the axial ligands, which may have relatively high intensity at the expense of the axial N−N stretching mode intensities. Indirect support for this assignment comes from a theoretical study of the iron dinitrogen complexes $Fe(NN)_{1-5}$.[38] The $a_2''$ dinitrogen stretching mode in $Fe(NN)_5$ is predicted to have less than one-seventh the intensity of the e′ mode, and is only slightly higher in intensity than the $a_2''$ metal−dinitrogen stretching mode. It is likely that the results are similar for the other metals in the iron group, and only a small error in the calculation or a small perturbation by the surrounding matrix would be required to alter the intensities of the high and low frequency $a_2''$ modes such that only the lower $a_2''$ mode is observable.

When osmium is co-deposited with nitrogen in argon, bands are observed at 2083.1 $cm^{-1}$ (C, Figure 5) and 2044.2 $cm^{-1}$ (A, Figure 5), with $^{15}N_2$ counterparts at 2013.9 and 1976.2 $cm^{-1}$. Both bands are diminished on annealing and on photolysis. The 2083.1/2013.9 $cm^{-1}$ pair has an intermediate band at 2033.8 $cm^{-1}$ in the mixed isotopic experiment with approximately twice the intensity of the pure isotope peaks, indicating that two dinitrogen units are involved in the vibration. These bands are therefore assigned to $Os(NN)_2$. No intermediate bands are observed for the 2044.2/1976.2 $cm^{-1}$ pair in the mixed isotope experiment, and these bands are assigned to the mono dinitrogen complex Os(NN). An intense band grows in strongly during annealing at 2138.9 $cm^{-1}$ (E, Figure 5), with a $^{15}N_2$ counterpart at 2067.6 $cm^{-1}$. The spectra are too congested to be able to identify the intermediate components in the mixed isotopic experiment, but these bands must correspond to the highest coordination complex and are therefore assigned to $Os(NN)_5$, blue shifted by 19 $cm^{-1}$ with respect to the nitrogen matrix value. Other bands grow in at 2106.0 $cm^{-1}$ (D, Figure 5), 2070.0 $cm^{-1}$ (B, Figure 5), and 2186.8 $cm^{-1}$ (F, Figure 5) on annealing, but the $^{15}N_2$ counterparts or intermediate components could not be determined due to spectral congestion. However, $Os(NN)_3$ and $Os(NN)_4$ must be present, and the bands B and D, respectively, are tentatively assigned to these species. No assignment is suggested for the band at 2186.8 $cm^{-1}$. If it tracked with the 2138.9 $cm^{-1}$ band, it could be due to the out-of-phase stretching mode of the axial ligands in $Os(NN)_5$, but this is not the case.

When ruthenium is co-deposited with pure nitrogen, intense bands are observed at 2151.2, 2149.3, 2147.5 and 2147.0 $cm^{-1}$ which are due to a ruthenium dinitrogen complex in different matrix sites. The $^{15}N_2$ counterparts for these bands are at 2079.6, 2077.6, 2076.1, and 2075.5 $cm^{-1}$ respectively giving isotopic ratios that are typical for dinitrogen complexes. These bands decrease on annealing and photolysis. When the experiment is repeated with a $^{14}N_2$ + $^{15}N_2$ mixture what look like three intermediate bands are observed at 2121.6, 2099.5, and 2087.0 $cm^{-1}$ which are less intense than either of the pure isotope bands (Figure 4). The lowest frequency component at 2087.0 $cm^{-1}$ is probably not an intermediate component, and these bands are assigned to the degenerate stretching mode in $Ru(NN)_5$, analogous to osmium. The second dinitrogen stretching mode expected for this molecule is not observed, but a band that gives a 1:2:1 triplet in the mixed isotopic experiment is observed at 499.0 $cm^{-1}$ that tracks with the high-frequency bands, also analogous to the osmium dinitrogen system.

When ruthenium is co-deposited with nitrogen in argon (Figure 6), prominent bands are observed at 2034.6 (A), 2077.6 (B), 2091.2 (C), 2126.5/2119.3 (D), and 2148.8 $cm^{-1}$ (E), with $^{15}N_2$ counterparts at 1967.1, 2008.6, 2053.0, and 2077.3 $cm^{-1}$. No intermediate bands are observed for the 2034.6/1967.1 $cm^{-1}$ pair, and these bands are assigned to Ru(NN). The spectra are too confused to be able to identify intermediate components for the other bands, but it is quite likely that these correspond to $Ru(NN)_2$, $Ru(NN)_3$, $Ru(NN)_4$, and $Ru(NN)_5$ as the latter species absorbs at essentially the same frequency in argon as in pure nitrogen.

This discussion provides a reasonable interpretation of the dinitrogen complex observations, but without further information many of these assignments are only tentative, and a more thorough study of the osmium and ruthenium dinitrogen complexes will be required before more definitive assignments can be made.

## Conclusions

Laser-ablated osmium and ruthenium atoms were reacted with nitrogen molecules to form the diatomic and triatomic nitrides MN and NMN and numerous dinitrogen complexes $M(NN)_n$. *Osmium is observed to insert into the dinitrogen bond on annealing in the cold matrix*, which shows that Os will be a good nitrogen fixation catalyst and allows a lower limit on the average Os−N bond enthalpy in NOsN to be established, namely, $\geq 0.5 \times D(N{\equiv}N)$. DFT calculations were effective in reproducing the experimental observations for the nitride and dinitrides, but further investigation of the dinitride molecules will be useful. Comparison of the force constants in the iron group for MN and NMN show that the bonds get stronger moving down the group from iron to ruthenium to osmium, the diatomic force constants are greater than those for NMN by ∼18% for ruthenium and osmium. Complexation of the diatomic molecules by dinitrogen reduces the force constants in OsN and RuN considerably. Examination of the MN and NMN molecules using NBO analyses show that the nitrides are all covalently

bound with triple bonds, except for NRuN which has Ru−N bond orders of 2.5.

Dinitrogen complexes are observed for both metals, and on the basis of the mixed isotopic frequency and intensity patterns the most highly coordinated complexes in pure nitrogen are probably $Os(NN)_5$ and $Ru(NN)_5$, analogous to the pentacarbonyl complexes already known for these metals.

**Acknowledgment.** We gratefully acknowledge N.S.F. support for this research under Grant CHE 97-00116.

## References and Notes

(1) Cotton, S. A. *Chemistry of Precious Metals*; Blackie Academic and Professional: 1997.

(2) Pell, S.; Mann, R. H.; Taube, H.; Armor, J. N. *Inorg. Chem.* **1974**, *13*, 479.

(3) Love, J. L.; Robinson, W. T. *Inorg. Chem.* **1972**, *11*, 1662.

(4) Dietrich, H.; Geng, P.; Jacobi, K.; Ertl, G. *J. Chem. Phys.* **1996**, *104*, 375.

(5) Matsushima, T. *Surf. Sci.* **1988**, *197*, L287.

(6) King, D. A.; Woodruff, D. P. *The Chemical Physics of Solid Surfaces*; Elsevier: New York, 1993; Vol. 6.

(7) Chertihin, G. V.; Andrews, L.; Neurock, M. *J. Phys. Chem.* **1996**, *100*, 14609.

(8) Burkholder, T. R.; Andrews, L. *J. Chem. Phys.* **1991**, *95*, 8697.

(9) Chertihin, G. V.; Andrews, L. *J. Chem. Phys.* **1995**, *99*, 6356.

(10) Frisch, M. J.; Trucks, G. W.; Schlegel, H. B.; Scuseria, G. E.; Robb, M. A.; Cheeseman, J. R.; Zakrzewski, V. G.; Montgomery, J. A., Jr.; Stratmann, R. E.; Burant, J. C.; Dapprich, S.; Millam, J. M.; Daniels, A. D.; Kudin, K. N.; Strain, M. C.; Farkas, O.; Tomasi, J.; Barone, V.; Cossi, M.; Cammi, R.; Mennucci, B.; Pomelli, C.; Adamo, C.; Clifford, S.; Ochterski, J.; Petersson, G. A.; Ayala, P. Y., Cui, Q.; Morokuma, K.; Malick, D. K.; Rabuck, A. D.; Raghavachari, K.; Foresman, J. B.; Cioslowski, J.; Ortiz, J. V.; Stefanov, B. B.; Lui, G.; Liashenko, A.; Piskorz, P.; Komaromi, I.; Gomperts, R.; Martin, R. L.; Fox, D. J.; Keith, T.; Al-Laham, M. A.; Peng, C. Y.; Nanayakkara, A.; Gonzalez, C.; Challacombe, M.; Gill, P. M. W.; Johnson, B.; Chen, W.; Wong, M. W.; Andres, J. L.; Gonzalez, C.; Head-Gordon, M.; Replogle, E. S.; Pople, J. A. *Gaussian 98*, Revision A.6; Gaussian, Inc.: Pittsburgh, PA, 1998.

(11) Lee, C.; Yang, E.; Parr, R. G. *Phys. Rev. B* **1988**, *37*, 785.

(12) McLean, A. D.; Chandler, G. S. *J. Chem. Phys.* **1980**, *72*, 5639. Krishnan, R.; Binkley, J. S.; Seegar, R.; Pople, J. A. *J. Chem. Phys.* **1980**, *72*, 650.

(13) Hay, P. J.; Wadt, W. R. *J. Chem. Phys.* **1985**, *82*, 299.

(14) Ram, R. S.; Lievin, J.; Bernath, P. F. *J. Chem. Phys.* **1999**, *111*, 3449.

(15) Ram, R. S.; Lievin, J.; Bernath, P. F. *J. Chem. Phys.* **1998**, *109*, 6329.

(16) Andrews, L.; Bare, W. D.; Chertihin, G. V. *J. Phys. Chem. A* **1997**, *101*, 8417.

(17) Zhou, M.; Andrews, L. *J. Chem. Phys. Chem. A* **1998**, *102*, 9061.

(18) Citra, A.; Andrews, L. *J. Phys. Chem. A* **1999**, *103*, 3410.

(19) Andrews, L. *J. Electron. Spectrosc.* **1998**, *97*, 63.

(20) Bytheway, I.; Wong, M. W. *Chem. Phys. Lett.* **1998**, *282*, 219.

(21) Collman, J. P.; Hegedus, L. *Principles and Applications of Organo Transition Metal Chemistry*; University Science Books: Menlo Park, CA, 1980.

(22) Tain, R.; Facelli, J. C.; Michl, J. *J. Phys. Chem.* **1988**, *92*, 4073.

(23) Huber, K. P.; Herzberg, G. *Constants of Diatomic Molecules*; van Nostrand Reinhold: New York, 1979.

(24) Allavena, M.; Rysnik, R.; White, D.; Calder, V.; Mann, D. E. *J. Chem. Phys.* **1969**, *50*, 3399.

(25) Green, D. W.; Ervin, K. M. *J. Mol. Spectrosc.* **1981**, *88*, 51.

(26) Van Zee, R. J.; Hamrick, Y. M.; Li, S. Weltner, W., Jr. *J. Phys. Chem.* **1992**, *96*, 7247.

(27) Andrews, L.; Souter, P. F.; Bare, W. D.; Liang, B. *J. Phys. Chem. A* **1999**, *103*, 4649.

(28) Wilson, E. B., Jr.; Decius, J. C.; Cross, P. C. *Molecular Vibrations*, Dover Publications: New York, 1955.

(29) Herzberg, G. *Spectra of Diatomic Molecules*, D. Van Nostrand, Princeton, NJ, 1950. The present upper limit estimate for $D_e$(OsN) is above a lower limit value (616 kJ/mol) calculated by Lievin using the MRCI method described in ref 14.

(30) Chertihin, G. V.; Bare, W. D.; Andrews, L. *J. Phys. Chem. A* **1998**, *102*, 3697.

(31) Reed, A. E.; Curtiss, L. A.; Weinhold, F. *Chem. Rev.* **1988**, *88*, 899.

(32) Neuhaus, A.; Veldkamp, A.; Frenking, G. *Inorg. Chem.* 1994, *33*, 5278.

(33) Willson, S.; Andrews, L. *J. Phys. Chem. A* **1999**, *103*, 1311.

(34) Darling, J. H.; Ogden, J. S. *J. Chem. Soc., Dalton. Trans.* **1972**, *No 3*, 2496.

(35) Calderazzo, F.; L' Eplattenier, F. *Inorg. Chem.* **1967**, *6*, 1220.

(36) Rushman, P.; van Buuren, G. N.; Shiralian, M.; Pomeroy, R. K. *Organometallics* **1983**, *2*, 693.

(37) Collman, J. P, Hegedus, L. S.; Norton, J. R.; Finke, R. G. *Principles and Applications of Organotransition Metal Chemistry*; University Science Books: Mill Valley, CA, 1987.

(38) Duarte, H. A.; Salahub, D. R.; Haslett, T.; Moskovits, M. *Inorg. Chem.* **1999**, *38*, 3895.